Synthesis and characterization of hematite biocomposite using cassava starch template for aqueous phase removal of fluoride

Article · August 2022

DOI: 10.1016/j.carpta.2022.100241

CITATIONS
0

READS
42

6 authors, including:

Walter Ojok
MUNI University
8 PUBLICATIONS **35** CITATIONS
SEE PROFILE

Emmanuel Ntambi
Mbarara University of Science & Technology (MUST)
24 PUBLICATIONS **85** CITATIONS
SEE PROFILE

James P. Bolender
University of San Diego
22 PUBLICATIONS **657** CITATIONS
SEE PROFILE

John Wasswa
Makerere University
13 PUBLICATIONS **155** CITATIONS
SEE PROFILE

Some of the authors of this publication are also working on these related projects:

Graduate Research Projects View project

Geochemistry of fluoride contamination in Ndali- Kasenda Crater lakes View project

Carbohydrate Polymer Technologies and Applications 4 (2022) 100241

Contents lists available at ScienceDirect

Carbohydrate Polymer Technologies and Applications

journal homepage: www.sciencedirect.com/journal/carbohydrate-polymer-technologies-and-applications

Synthesis and characterization of hematite biocomposite using cassava starch template for aqueous phase removal of fluoride

Walter Ojok [a,b,f,*], Emmanuel Ntambi [a], James Bolender [c], John Wasswa [d], William Wanasolo [e], Brenda Moodley [f]

[a] Department of Chemistry, Faculty of Science, Mbarara University of Science and Technology, P.O Box 1410, Mbarara, Uganda
[b] Department of Chemistry, Faculty of Science, Muni University, P.O Box 725, Arua, Uganda
[c] Department of Chemistry and Biochemistry, University of San Diego, 5998 Alcala Park, San Diego, CA 92110, United States America
[d] Department of Chemistry, College of Natural Sciences, Makerere University, P.O Box 7062, Kampala, Uganda
[e] Department of Chemistry, Faculty of Science, Kyambogo University, P.O Box 1 Kyambogo, Kampala, Uganda
[f] School of Chemistry and Physics, University of KwaZulu-Natal, Westville Campus, Durban, 4000, South Africa

ARTICLE INFO

Keywords:
Cassava starch
Hematite
Fluoride sorption
Kinetics
Equilibrium isotherm
Response surface methodology

ABSTRACT

In this study, facile synthesis of α-Fe_2O_3 biocomposite was mediated by cassava starch as a soft template. Batch mode evaluated its sorption behavior for fluoride removal from aqueous media. Characterization studies using analytical techniques confirmed the existence of porous α- Fe_2O_3 biocomposite with heterogeneous surfaces having a varied affinity for fluoride. The sorption process was optimized using central composite design (CCD) in response surface methodology (RSM) with a good model prediction ($R^2 = 0.9066$). A study of the interaction effect showed the synergy of process variables on fluoride removal with the result's intensity indicated by the nature of contour plot curvature. Based on the RSM optimization, an optimum fluoride removal efficiency of 85.26 % can be achieved at an initial fluoride concentration of 55 mg/L, α- Fe_2O_3 biocomposite dose of 0.55 g, pH of 7.5, and contact time of 95 min. Sorption equilibrium data were well modeled by Freundlich isotherm (0.9916), indicating multilayer sorption on a heterogeneous surface of the sorbent with a varied affinity for fluoride. Presence of co-existing anions reduced fluoride removal efficiency in the order $PO_4^{3-} > HCO_3^- > SO_4^{2-} > NO_3^- > Cl^-$. At the same time, its kinetics was better modeled by pseudo-second-order kinetics ($R^2 = 0.9764$), showing that the sorption process is rate-limiting. The sorption thermodynamics study showed that the process was spontaneous, exothermic, and entropy-driven physisorption. Hence, the results signify that the green synthesized α- Fe_2O_3 biocomposite could be a potential sorbent for sustainable defluoridation.

1. Introduction

The green chemistry approach to the synthesis of iron oxide nanoparticles has garnered much scientific research due to its enormous applications in catalytic, medical, and environmental remediation, development of sensors, electrodes, and magnetic storage devices (Hoque et al., 2019; Raghav & Kumar, 2019; Xu et al., 2017). Furthermore, the superior physicochemical characteristics of iron oxide polymorphs and their composites make them suited for numerous applications. For example, Hoque et al.(2019) and Murambasvina & Mahamadi (2020) reported efficient sequestration of inorganic pollutants from water employing iron oxides and their composites synthesized from biopolymers, including starch, cellulose, and alginates. In addition, these materials have higher sorption efficiency and stability than biopolymers alone (Hegde et al., 2020). Consequently, research into the synthesis and application of composites with metal oxides/ metal oxyhydroxides entrapped into the matrices of biopolymers has gained momentum over the last decades(Mondal & Purkait, 2019; Singh et al., 2018). Furthermore, composites containing metal oxides/ oxyhydroxides dispersed into the biopolymer matrices have shown great potential in removing dyes, metal ions, and anionic pollutants such as fluoride from water (Abbo et al., 2021; Hegde et al., 2020; Sasireka &

Abbreviations: RSM, Response surface methodology; CCD, Central Composite Design; CS, Cassava starch; ICP-OES, Inductively Coupled Plasma- Optical Emission Spectrometer; TEM, Transmission electron microscope; SEM, Scanning electron microscope; EDS, Energy dispersive spectroscopy; XRD, X-ray powder diffractometer; FTIR, Fourier-transformed infrared spectrometer; BET, Brunauer-Emmett-Teller; BJH, Barrett-Joyner-Halenda.

* Corresponding author.
E-mail address: w.ojok@muni.ac.ug (W. Ojok).

https://doi.org/10.1016/j.carpta.2022.100241

Available online 24 August 2022

Lalitha, 2021).

Xu et al.(2017) entrapped Zr^{4+} onto porous starch biopolymer and reported a remarkable maximum defluoridation capacity of 25.41 mg/g over a wide pH range. This study reveals the extraordinary ability of metal oxide/oxyhydroxide biocomposite from starch to remove fluoride and other pollutants from aqueous media.

Fluoride is a globally distributed contaminant occurring in groundwater, affecting over 200 million people in some 28 countries (Ojok et al., 2021; Wang, 2020). Ingestion of fluoride-rich water is a significant route of fluoride entry into the human body. At low concentrations (< 1.5 ppm), fluoride is essential for the healthy human mineralization of skeletal structures. However, a high fluoride concentration can cause several health problems, including dental and skeletal fluorosis, neurological and digestive disorders, decreased fertility, and lowered human intelligence (Alhassan et al., 2020; Erdal & Buchanan, 2005). Such health risks make fluoride contamination a public health risk worldwide, requiring amelioration strategies.

Mumtaz et al. (2015) and other researchers reported fluoride removal from water using several methods, including chemical precipitation, reverse osmosis, ion exchange, nano-filtration, electro-dialysis, surface adsorption, and electrolysis. Due to its high efficiency and pecuniary advantage, the sorption technique is favorably chosen (Gupta et al., 2021). However, suitable sorbents must be available for sorption to be economically viable. Therefore, many sorbents, including carbon nanotubes, metal oxides/hydroxides, their composites, resins, industrial solid wastes, agricultural waste-based materials, and natural minerals, have been utilized(Abbo et al., 2021; Raghav & Kumar, 2019). Though agricultural waste-based sorbents are of low cost, their efficiency is limited since regeneration is a challenge(Egor et al., 2021; Gautam et al., 2019; Prabhu & Meenakshi, 2015; Raghav& Kumar, 2019).

Herein, we report an ecologically friendly method for scalable and economical production of α.Fe_2O_3 composite using cassava starch as a soft template by incorporating α-Fe(OOH) moieties into the cassava starch matrix. Starch is one of the most attractive biopolymer that is widely used in the food industry and nanotechnology(Visinescu et al., 2010). In this research, the starch was obtained from cassava waste, produced by scrubbing off the outer part of peeled cassava tuber during cassava preparation for food in Uganda. Although starch serves as a protecting, hosting, binding, structure tailoring, and separating agent in nanotechnology, it quickly disperses in water when alone, even in a calcined form. However, when a lewis acid like Fe^{3+} is co-precipitated in the starch matrix, it affords numerous benefits to the composite(Visinescu et al., 2010). Again, it is easier to remove the starch template than other sol-gel chelating agents such as ethylenediamine tetra acetic acid and citric acid, by calcination at a lower temperature(Shah et al., 2022). Xu et al.(2017) successfully incorporated Zr^{4+} into porous starch matrices for effective fluoride removal from water. However, such rare earth metals are usually precarious, making sorbent production expensive for water treatment. Iron is relatively abundant and less costly than other metals such as Ce, La, and Zr. Fe^{3+} is a strong lewis acid and easily attracted to electron-rich species. Several iron oxide/oxyhydroxides and their composites have been utilized in the sequestration of pollutants from water(Fardood et al., 2017; Hoque et al., 2019). By increasing active sites, incorporating the FeOOH into starch matrices improves its fluoride removal ability. Again, the iron oxyhydroxide in the composite affords it rigidity and high surface area due to its high charge density numerous coordination sites for bonding(Shah et al., 2022). Hence, α-Fe_2O_3 can be used as a less resource-intensive material for fluoride removal from water. This study also investigated the effect of cassava *(Manihot esculenta Crantz)* starch on the growth, size, and shape of the α-Fe_2O_3 composite. The efficiency of the synthesized α-Fe_2O_3 biocomposite for aqueous phase removal of fluoride was also evaluated in batch experiments to contribute to the search for an efficient sorbent for sustainable fluoride removal from water. The physicochemical attributes of the as-synthesized α.Fe_2O_3 biocomposite were studied using standard analytical instruments before and after fluoride sorption to understand the sorption mechanism. The interactive effect of pH, contact time, initial fluoride concentration, and sorbent dose on fluoride removal efficiency was determined using the classical Central Composite Design (CCD) at different process conditions and a multivariate quadratic regression model developed to optimize the process.

2. Materials and methods

2.1. Materials

All chemicals were of analytical grade and were used without further purification. Sodium hydroxide, sodium fluoride (NaF), iron (III) chloride ($FeCl_3$), and nitric acid (HNO_3, 36 %) were purchased from Sigma Aldrich Co. USA, and the total ionic strength adjustment buffer (TISAB) from HACH company. Sodium chloride ($NaCl$), sodium nitrate($NaNO_3$), sodium sulfate (Na_2SO_4), potassium hydrogen carbonate ($KHCO_3$), and sodium phosphate (Na_3PO_4) were purchased from Loba Chemie Pvt.Ltd., India. Deionized water with electrical conductivity ~0.05 μS/cm was used for the preparation of solutions.

Fresh edible cassava *(Manihot esculenta Crantz)* tubers were obtained from a local market in Gulu City, Northern Uganda. The outer surface of peeled cassava tubers was carefully scrubbed with a cleaned knife and dried in an oven at 105 °C for 3 h and subsequently ground into a fine powder using a ball mill, further dried at 80 °C for 36 h, and stored in airtight glass containers for further studies.

A fluoride stock solution containing 100 mg/L was prepared by dissolving 0.221 g of anhydrous sodium fluoride in deionized water and made up to 1000 mL of solution. Serial dilutions were used to obtain the desired concentration of the fluoride test solution for the sorption study. Residual fluoride was determined using a Platinum series fluoride electrode (Model 51,928–88, HACH Co., Ltd, Loveland, Colorado, U.S. A).

2.2. Synthesis of α-Fe_2O_3 biocomposite

α.Fe_2O_3 biocomposite were synthesized by sol-gel method with cassava starch acting as a soft template. Iron (III) chloride (10 g) was added to deionized water (250 mL) and constantly stirred to dissolve. To this, 0.01 M sodium sulfate (10 mL) was added, and the mixture was magnetically shaken at 180 rpm for 5 min, followed by 20% cassava starch solution (10 mL) with constant stirring for another 5 min. Sodium hydroxide solution (4.0 M) (about 10 mL) was added drop-wise under vigorous stirring until its pH reached 10. The resultant dense brown precipitate was allowed to age for 12 h at room temperature in an incubator. The precipitate was then washed until pH 7 using deionized water to remove excess sodium hydroxide. The brown residue obtained by filtration was dried in an oven at 105 °C for 12 h and ground into a fine powder using a mortar and pestle. It was finally heated in a furnace at 600 °C for 3 h and allowed to cool in an airtight furnace for 12 h to give the α.Fe_2O_3 composite. The optimized protocol for synthesizing α-Fe_2O_3 biocomposite above was arrived at after adding 0, 5, and 20 mL of the starch solution to the same volume of ferric chloride solution and sodium sulfate or sodium phosphate (stabilizing agent) in separate experiments. The effect of cassava starch and stabilizing agent concentration on the physical properties of the composite was studied. In each case, a sample (1 g) of the powdered sorbent was shaken with deionized water to investigate its stability. Sodium sulfate solution was a better binder than sodium phosphate because its composite had almost the same fluoride removal performance as sample prepared without a binder. These and fluoride removal performances revealed that the optimum cassava starch concentration for maximum fluoride removal capacity with good stability was 10 mL of 20% cassava starch solution. Hence 10 mL of the 20% cassava starch solution was used to produce α-Fe_2O_3 biocomposite for the fluoride sorption study.

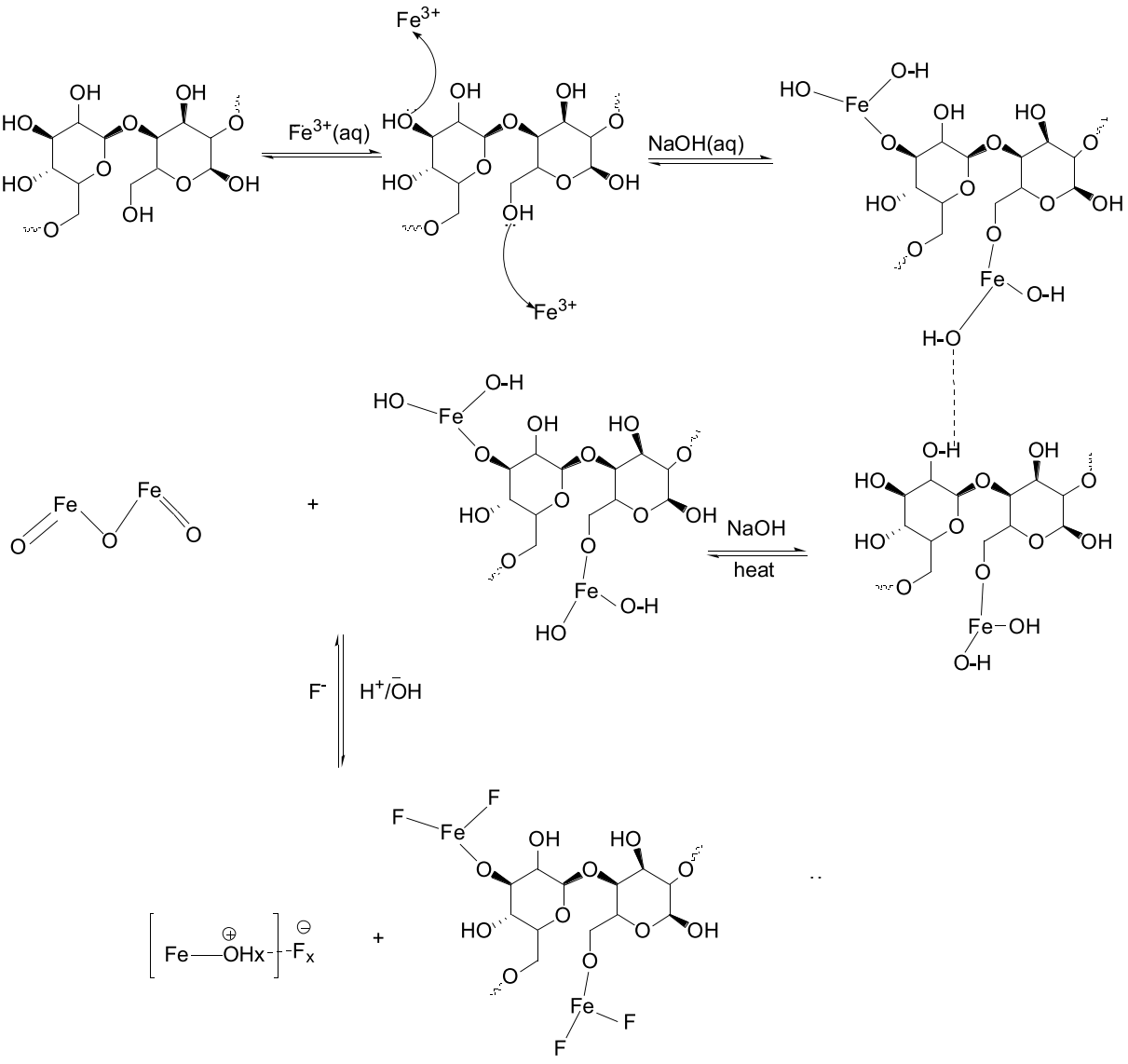

Fig. 1. Proposed mechanism for the formation of α-Fe_2O_3 composite and its fluoride removal mechanism.

2.3. Characterization of Fe_2O_3 biocomposite

The surface texture and morphology of the α-Fe_2O_3 biocomposite were studied using a scanning electron microscope (FESEM, ZEISS, Germany) at an accelerating voltage of 5 kV and a transmission electron microscope (HRTEM, JEOL-1230). At the same time, the elemental composition was analyzed using Energy Dispersive Spectroscopy. The phase composition and crystal structure were characterized by an X-ray powder diffractometer (XRD, D8 ADVANCE X, Germany) using Cu Kα (40 kV, 40 mA) radiation in the scanning range of 10–80. The Fourier-transformed infrared spectrometer (Perkin Elmer, UK equipment) was used to study the chemical structure of the composites in the wave-number range 400 – 4000 cm^{-1}. The Brunauer-Emmett-Teller (BET) and the Barrett-Joyner-Halenda (BJH) equations from the nitrogen adsorption-desorption isotherms determined by Micro metrics Tristar II surface area and porosity analyzer were used to calculate the surface area and pore size distribution of the α-Fe2O3 biocomposite. The leaching of iron metal into the treated water was gauged using the Perkin Elmer Optima 7300 DV Inductively Coupled Plasma- Optical Emission Spectrometer (ICP-OES) following the standard US EPA method 200.7.

2.4. Sorption experiments

Batch sorption experiments were performed using the as-synthesized α-Fe_2O_3 biocomposite to evaluate their sorption efficiency in removing fluoride from water. All experiments were performed using a 50 mL fluoride solution with independent factors: initial fluoride concentration, pH, sorbent dose, and contact time varied as described in Section 2.5. A given amount of sorbent was added to the fluoride solution in a 100 mL conical flask, then sealed and shaken at a constant speed of 180 rpm. The desired pH was adjusted using 0.1 M NaOH and 0.1 M HCl solutions. The solution was then separated by gravity filtration using Whatman number 1 filter paper (0.45 μm, Whatman, USA), and residual fluoride was analyzed using a fluoride ion-selective electrode. The experiments were done in triplicate, and average values were reported to ensure reproducibility.

Kinetic sorption experiments were carried out using 50 mL of a 55 mg/L fluoride solution and 0.5 g of sorbent magnetically shaken at 180 rpm at 0, 20, 40, 60, 80, 100, 140, 180, 220, 260, 300, 360 min. Equilibrium isotherm experiments were performed with 0.5 g of sorbent but different initial fluoride concentrations of 10, 20, 30, 40, 50, 60, 70, 80, 90, 100 mg/L for 24 h. Thermodynamic sorption experiments were performed using 0.5 g of sorbent and 50 mL of 55 mg/L of fluoride

solution at 293, 303, 313, and 323 K.

For the reusability study, sorbent (2 g) was initially shaken at 180 rpm with 10 mg/L of a fluoride solution for 12 h to attain equilibrium, and residual fluoride was determined as described earlier. After the sorption experiment in the first cycle, the spent sorbent was separated by centrifuging, and the residue was agitated with 0.1 M NaOH solution for 60 min. Finally, the residue was dried at 110 °C and used in additional sorption tests using the same procedure described in this section. The sorbent was regenerated four times in this experiment, each replicated three times.

2.5. Response surface methodology (RSM) study

The efficiency of fluoride sorption using as-synthesized α- Fe_2O_3 biocomposite and interactions between sorption process parameters were investigated using the Central Composite Design model (CCD). The sorption of fluoride on the prepared iron oxide composite highly depended on initial fluoride concentration (10–100 mg/L), solution pH (3–12), contact time (10 –180 min), and sorbent dose (0.1–1.0 g) Table S1(Supplementary material). The magnitude of each of these factors could affect the sorption process, with possible synergistic effects of the variables. Therefore, with different ranges of each variable, there will be different permutations and combinations to conduct experiments. Response surface methodology (RSM) enables the systematic design of an experimental matrix, which minimizes wastage by using fewer experiments and cannot be underscored in the overall process. In this study, CCD in Design-Expert Software (Version 13.0.0, Stat-Ease Inc. Minneapolis, Minnesota, USA) was used to model the interactive effects of the four independent variables on the removal efficiency of fluoride ions by the as-synthesized α- Fe_2O_3 biocomposite. Central composite design (CCD) was selected because it is a classical 5-level design for process optimization with excellent statistical properties (Dehghani et al., 2021; Lingamdinne et al., 2020). Overall, 30 experiments were conducted, representing the different space types in a cubical representation. The interaction between independent sorption process variables on the removal efficiency and optimum conditions for maximum fluoride removal efficiency was studied. A multivariable data-driven model was identified to predict fluoride removal efficiency for different ranges of the sorption process variables.

3. Results and discussion

3.1. Synthesis and characterization of α- Fe_2O_3 biocomposite

SEM images obtained in Fig. 2(a) and 2(b) showed the critical role played by the cassava starch in this study during the synthesis of α-Fe_2O_3 biocomposite. To optimize cassava starch concentration for mass production of composite used in this study, sorbent prepared at 0, 5, 10, and 20 mL of cassava starch (20%) was added to 10 mg/L of a fluoride solution. For the sample from 0 mL cassava starch, poor stability with higher fluoride removal efficiency (89.07%) was observed. Furthermore, increased cassava starch concentration from 0–20 mL led to a slight decrease in fluoride sorption efficiency from 89.07% to 82.01%, but textural properties improved significantly (Table S2) (supplementary material).

In the absence of cassava starch, irregularly shaped, less stable α-Fe_2O_3 particles were formed, as shown in Fig. 2(a). In the presence of starch, tubular and spherical shapes of α- Fe_2O_3 biocomposite were formed. The result indicates the potential role structure directing role of cassava starch and scaffolding α-FeOOH in its polymer framework. TEM images (Fig. 2(d)) showed that the size of the particles was in the range of 20 nm to 200 nm in diameter and length, respectively. The main elemental composition in the composite was Fe (20.26 %), C (30.66 %), and O (36.56 %). The iron and oxygen observed in the EDX spectrum before sorption (Fig 2 (e – j) are the elements present in the α- Fe_2O_3 biocomposite, while the residual carbon (Fig 2 e & h) and Na (2 e & j) may be from the starch and NaOH used as a soft template in the synthesis. Since only ferric chloride, cassava starch, and sodium hydroxide were used, no harmful chemicals were produced as by-products.

A possible mechanism (Fig. 1) for forming α-Fe_2O_3 composite involves the lone pairs of electrons of the polyol groups from the long chain starch biopolymers consisting of amylose and amylopectin polysaccharides(Visinescu et al., 2010). $Fe(OH)_3$ colloids got entrapped through hydrogen bonding in the numerous hydroxyl groups on the helical polysaccharide chains to form cage-like structures. In the absence of starch, movement of the entrapped $Fe(OH)_3$ is hindered, and aggregation of the colloids occurs to form a large mass of particles. However, in the presence of starch, two interactions may occur, $Fe(OH)_3$ - starch interaction and $Fe(OH)_3$ - $Fe(OH)_3$ via hydrogen bonding due to the structure-directing role of starch leading to the formation of a well-defined inclusion complex(Shah et al., 2022; Visinescu et al., 2010). Also, some of the α-1,4-glycosidic and α-1,6-glycosidic bonds underwent hydrolysis and oxidation in presence of ferric chloride to form shorter oligosaccharide chains and gluconic acid(Visinescu et al., 2010).

Calcinating the inclusion complex at 600 °C resulted in the pyrolysis of starch, yielding carbon dioxide and water. At the same time, $Fe(OH)_3$ moieties transformed to α-Fe_2O_3. Hence, Fe-O were formed during the calcination of adjacent $Fe(OH)_3$ moieties, and in the process, carbon dioxide and water are also formed. Additionally, the presence of cassava starch played an essential part in hosting the Fe^{3+}, controlling the shape as well as textural properties of the composite by causing anisotropic growth in specific directions to form rigid hexagonal and tubular biocomposite. Therefore, the formation of Fe_2O_3 indicates cassava starch's potential role in forming a well defined α-Fe_2O_3 composite that is stable in water.

Consequently, the main products formed in this synthesis are α-Fe_2O_3, H_2O, NaCl, and carbon dioxide. The SEM image of the as-synthesized α-Fe_2O_3 biocomposite reveals a rough surface morphology and wide-ranging size distribution averaging 200 nm. The roughness of the surface of the composite provided active sites for fluoride binding (He et al., 2020).

The wide-angle XRD spectra of the composites were measured using the D8 Advance to obtain information regarding its crystallinity and structure, displayed in Fig. 3(A).

The major reflection peaks observed at 2θ values at 31.7°, 35.2°, 56.5°, 62.8°, and 66.3° correspond to the planes of (104), (110), (116), (214), (018), and (300) of crystalline α-Fe_2O_3 (JCPDS 33–0664) (Fardood et al., 2017; Hoque et al., 2019). The additional peaks at 2θ values at 45.7° and 75.3° correspond to the diffraction planes of (510) and (622) of Fe_3O_4 (JCPDS 19–0629)(Zhang et al., 2016). Further, the d-spacing values obtained are similar to those of the International Center for Diffraction Data (ICDD), showing the presence of α-Fe_2O_3 and Fe_3O_4 in the composite.

The average crystallite size of the composite was determined from the Scherrer formula (Eq. 1) using the full width at half maximum (FWHM) of the most intense peak.

$$D = \frac{k\lambda}{\beta cos\theta} \quad (1)$$

where 2θ = 31.7624 for the most intense peak at the diffraction plane (104), θ = Bragg's diffraction angle, D = diameter of the crystallite size, k = 0.90, λ (1.5406 nm) = wavelength of the x-rays of the Cu Kα radiation, while β = FWHM.

The average crystal size of the composite calculated from the Scherer equation was 76.98 nm which is higher than that for hematite prepared using rice starch in a study by Hoque et al. (2019).

FTIR spectroscopy was employed in this study to investigate the role of starch in α-Fe_2O_3 composite synthesis and the mechanism of fluoride removal by the as-synthesized α-Fe_2O_3 composite. FTIR spectra of pure cassava starch, α-Fe_2O_3 prepared without starch, α-Fe_2O_3- cassava starch

composite, and α-Fe_2O_3 composite-fluoride are shown in Fig. 3 (B). The FTIR spectrum of pure cassava starch (Fig. 3 (B) (a)) showed characteristic broadband at 3200 – 3450 $cm^{-1,}$ corresponding to O-H bond stretching vibration (Hoque et al., 2019). After the cassava starch was added to the Fe^{3+} solution, the peak at 3440 cm^{-1} shifted to 3410 cm^{-1}, indicating an interaction of the Fe^{3+} ion with O-H groups in the polysaccharide. The peaks appearing at 1617 cm^{-1}, 1405 cm^{-1}, and 1324 cm^{-1} (Fig. 3 B (a) are due to asymmetric stretching vibrations of C-H, C-OH, and C-O-C bonds in the cassava starch, respectively (Egor et al., 2021; Xu et al., 2017). Masking by fluoride ions reduced the peak in the spectrum of the α-Fe_2O_3 biocomposite at 881 cm^{-1} after fluoride sorption Fig 3B(c) (Mahfoudhi & Boufi, 2020).

The prominent peaks that appeared between 630 cm^{-1} and 500 cm^{-1} (Fig. 3B(b, c, d) can be assigned to the Fe-O bond stretching vibrations (Fardood et al., 2017). The peaks at 1446 cm^{-1} and 885 cm^{-1} (Fig. 3 B (c) may be due to stretching vibrations of unreacted ketone groups. Sarkar et al. (2012). After the fluoride sorption, the peak at 3600 cm^{-1}shifted to 3287 cm^{-1}, indicating the involvement of the O-H group, and that at 632 cm^{-1} shifted to 510 cm^{-1} revealing electrostatic interaction in the removal of fluoride by the as-synthesized α-Fe_2O_3 biocomposite. The broad and prominent peak at 1000 cm^{-1} (Fig 3B (a) is assigned to the C-O-C of the α-1,4-glycosidic α-1,6-glycosidic bonds in starch. This peak became less prominent than for pure cassava starch when ferric chloride was added to the starch (Fig 3B (c). This may result from hydrolysis and oxidation of some of the α-1,4-glycosidic and α-1, 6-glycosidic bonds in the starch matrix in the presence of Fe^{3+}(Shah et al., 2022) which reduced the amount of C-O-C bonds in the composite. Hence the disappearance of the prominent peak at 881 cm^{-1}.

Pore size distribution and surface area of the as-synthesized α-Fe_2O_3 biocomposite were determined using the BET and BJH methods. The BET surface area of the as-synthesized α-Fe_2O_3 biocomposite was 1.0377 m^2/g with a BJH surface area of 1.3623 m^2/g. The BJH analysis showed that the average pore diameter and cumulative pore volume of the as-synthesized α-Fe_2O_3 composite were 72.3068 Å and 0.007028 cm^3/g, respectively, indicating its porous nature (Fig. 3 (C) and (D).

A critical look at Fig. 3 (C) reveals a Type III BET sorption isotherm with Type I hysteresis (Everett et al., 1974). This further indicates that the as-synthesized α-Fe_2O_3 composite is mesoporous with numerous multilayer sorption sites. Initially, sorption of N_2 increases at a low relative pressure of the gas, followed by the sorbent's interaction with less energetic gas molecules. After the completion of monolayer sorption, the formation of the multilayer starts to occur, leading to a sharp rise in the curve. The heterogeneity of the composite allowed stronger interactions between the multilayers than those within the monolayers of the as-synthesized α-Fe_2O_3 biocomposite (Egor et al., 2021; Everett et al., 1974). This explains the sorption behavior observed in this study which fitted better with the Freundlich isotherm.

3.2. Effect of pH on fluoride removal

Solution pH plays an integral role in the sorption of fluoride as it changes the surface charge of a sorbent and ionic species in the solution (Raghav & Kumar, 2019; Xu, Chen, Peng, Qiao, Ke, & Hou, 2017). This study studied the effect of solution pH on fluoride removal from aqueous solution using as-synthesized α-Fe_2O_3 biocomposite at pH values 3–12, Fig. 4 (a). At low pH ($3 \leq pH \leq 8$), there was a steady increase in fluoride removal efficiency by the as-synthesized α-Fe2O3 composite reaching a maximum in the pH range of 6 - 8. During low pH, there is protonation of the surface of as-synthesized α-Fe_2O_3 biocomposite in the weakly acidic media, which increases the number of active sites on its surface for electrostatic fluoride attraction (Egor et al., 2021; Prabhu & Meenakshi, 2015). As pH increased beyond 8, fluoride removal capacity decreased rapidly from pH 9.0 to 10 and then gradually reached its lowest value at pH 12. At pH 7–8, forming metallo-fluoro complexes on highly charged Fe^{3+} ions may explain the high fluoride sorption observed in this study (Tefera et al., 2020).

Table 1
Comparative evaluation of Langmuir sorption capacity of this present work with those of other iron oxide composites for fluoride removal in literature.

Sorbent	pH	Sorption capacity (mg/g)	Reference
Fe_2O_3 @ ionic liquid	7	67.9	Pillai, Dharaskar et al. (2020)
Fe_2O_3 @ Sand	6.01	2.04	Gogoi et al. (2018)
Fe-Al-La trioxide	8.25	28.06	Gasparotto et al. (2021)
Fe_2O_3@water hyacinth	3.0 – 6	4.18	Murambasvina & Mahamadi (2020)
Fe-Sn mixed oxide	5–7.5	10.5	Biswas et al. (2009)
β-FeOOH	4 – 8	7.0	Kumar et al. (2009)
Fe_3O_4@hydrotalcite	5	3.04	Pandi et al. (2017)
α-Fe_2O_3 biocomposite	6–8	3.2	This present work

In strongly alkaline pH media, the surface of the as-synthesized α-Fe_2O_3 biocomposite was saturated with negatively charged hydroxide ions. The strongly alkaline pH resulted in electrostatic repulsion of fluoride ions, restraining diffusion of fluoride ions onto the sorbent surface and consequently lowering fluoride removal efficiency. Our result concurs with other studies, which showed high fluoride sorption capacity using iron oxide-based sorbents at low pH and low sorption capacity in alkaline solution (Mondal & Purkait, 2019; Raghav & Kumar, 2019). Therefore, pH 7.5 was chosen as the optimum pH for sorptive removal of fluoride ions in further sorption studies.

3.3. Sorption equilibrium and isotherm study

The effect of initial fluoride concentration on the sorption process was investigated by carrying out batch sorption experiments at fluoride concentrations in the range of 10–100 mg/L and a fixed sorbent dose of 0.5 g.

The concentration of fluoride ions at equilibrium, Q_e (mg/g), on the sorbent surface was calculated according to Eq. (2).

$$Q_e = \frac{(C_o - C_{e)}}{w} V \tag{2}$$

Where Co and Ce (mg/L) are the initial and equilibrium concentration of fluoride ions in the solution, w (g) is the mass of α-Fe_2O_3 biocomposite used, and V (liters) is the volume of solution used.

As seen in Fig. 4 (b) sorption capacity, Q_e of the as-synthesized α-Fe_2O_3 biocomposite increased with an increase in initial fluoride concentration. This steady increase in sorption capacity is attributed to the availability of active sites which had not yet reached saturation. High fluoride concentration in the solution facilitates powerful interactions between the fluoride ions and sorbent. However, the rise in Q_e decelerated gradually at a higher initial concentration of fluoride ions (>80 (mg/L) due to the saturation of the active sites of the α-Fe_2O_3 biocomposite with fluoride ions. The decrease in Q_e at high fluoride concentration is consistent with earlier reports (Raghav & Kumar, 2019; Tang et al., 2018).

In order to understand the sorption behavior of fluoride ions onto the as-synthesized α-Fe_2O_3 biocomposite, the batch sorption data were modeled using Langmuir (1918); Freundlich (1906); Temkin & Pyzhev, 1940) isotherms. The equations in Table 2 adequately describe the three isotherms with the corresponding results obtained in this study.

For the Langmuir isotherm, the Q_m = maximum sorption capacity corresponding to monolayer coverage on the surface of the sorbent and K_b = Langmuir constant, which is related to the energy of sorption, were determined from the slope and the intercept of the plot in Fig 4(c). Again, another critical parameter in the Langmuir isotherm called the separation factor, R_L given by Eq. (3) was calculated

$$R_L = \frac{1}{(1 + K_b C_o)} \tag{3}$$

A value of $0 < R_L < 1$ shows a good uptake of the sorbed species. As

Table 2
Sorption isotherm parameters of fluoride using α-Fe_2O_3 biocomposite (N = 3, Relative standard deviation, RSD < 5%).

Isotherm	Equation	Parameter	Value
Temkin	$Q_e = BlnK_T + lnC_e$	B (J/mol)	0.6499
		R^2	0.9581
		K_T	2.49
Langmuir	$\frac{1}{Qe} = \frac{1}{K_b Q_m}\left(\frac{1}{Ce}\right) + \frac{1}{Q_m}$	Q_m (mg/g)	3.155
		K_b (L/mg)	0.20745
		R_L	0.32526
		R^2	0.9801
Freundlich	$Q_e = \ln K_F + \frac{1}{n} lnC_e$	K_F (mg/g) (L/mg)$^{1/n}$	3.410
		n	1.8941
		R^2	0.9916
		1/n	0.528

Definition of equation terms: Q_e = concentration of fluoride ions sorbed at equilibrium, C_e = equilibrium concentration of fluoride ions, R_L = separation factor, Q_m = maximum sorption capacity corresponding to monolayer coverage on the surface of sorbent, K_b = Langmuir constant, which is related energy of sorption, K_F and 1/n are Freundlich constants while K_T and B are Temkin constants

shown in Table 2, the R_L (0.325) value obtained in this study indicates that the binding of fluoride to the as-synthesized α-Fe2O3 composite is highly favorable, with a maximum sorption capacity, Q_m of 3.2 mg/g, and R^2 = 0.9801 (Egor et al., 2021; Raghav & Kumar, 2019). From Table 1, it can be seen that the sorption capacity achieved in this study was still higher than those reported for other iron oxide composites such as iron oxide-modified sand (2.04 mg/g) (Gogoi et al., 2018) and magnetic iron oxide coated hydrotalcite (3.02 mg/g) (Pandi et al., 2017).

The fluoride removal capacity of our composite is comparable with water hyacinth/hydrous iron oxide composite, with a sorption capacity of 4.18 mg/g (Murambasvina & Mahamadi, 2020).

For a heterogeneous system, the Freundlich isotherm is considered a suitable model. A linear form of the equation for the Freundlich isotherm is given in Table 2 with the calculated parameters obtained from a plot depicted in Fig. 4(d). The Freundlich constants 1/n and K_F were used to approximate the sorption capacity and strength of fluoride binding onto as-synthesized α-Fe_2O_3 biocomposite, respectively, as these constants are used to determine the characteristics of the sorbent-sorbate system. The values of 1/n obtained in this study indicated that favorable fluoride sorption occurred on the heterogeneous surfaces of the as-synthesized α-Fe_2O_3 composite with varied affinities for fluoride (R^2 = 0.9916) (Freundlich, 1906).

Similarly, the Temkin model that assumes a linear rather than logarithmic decrease for an intermediate sorbate concentration with coverage of the sorbate on the sorbent surface (Temkin & Pyzhev, 1940) was applied. In this study, the distribution of binding energies was evaluated using the equation in Table 2 and the linear plot given in Fig. 4 (e). The Temkin isotherm constant B was calculated using Eq. (4).

$$B = \frac{RT}{b} \tag{4}$$

Where R is the universal gas constant (8.314 J/mol/K), T is the absolute temperature (K), and b is a dimensionless Temkin isotherm constant related to the heat of sorption due to sorbent-sorbate interactions (Temkin & Pyzhev, 1940). The calculated Temkin parameters are presented in Table 2. The values obtained indicate that the enthalpy change associated with the binding of fluoride to the α-Fe_2O_3 biocomposite is favorable for the sorption of fluoride on the sorbent (Raghav & Kumar, 2019; Temkin & Pyzhev, 1940). Further scrutiny of the Temkin plot (Fig. 4 (e)) reveals two stages of the sorption process. Initially, the heat fall for the first three points was linear, while the next stage comprising 7 points, was non-linear. These results may point to the formation of a monolayer coverage when the initial concentration of fluoride is low (≥40 mg/L); however, multilayer sorption appears to manifest at higher initial fluoride concentrations (40–100 mg/L).

3.4. Sorption kinetic study

Fluoride sorption kinetics of as-synthesized α-Fe_2O_3 biocomposite was studied to decipher the sorption behavior. As seen in Fig. S5, initially, the sorption capacity increased rapidly due to free available active sites for fluoride binding at the beginning of the sorption process. Sorption equilibrium was reached at about 100 min with an initial fluoride concentration of 10 mg/L at 298 K. The Lagergren pseudo-first-order, pseudo-second-order, Weber-Morris intraparticle diffusion, and Elovich models were used to fit the sorption data to evaluate the sorbent's performance and investigate the sorption behavior of fluoride onto the as-synthesized α-Fe_2O_3 biocomposite.

Table 3
Kinetics parameters.

Sorption model	Parameters	Values	R^2
Weber- Moris	Q_e, exp. (mg/g)	1.0000	0.7654
	k_{id} (mg/g) (min$^{-0.5}$)	0.0370	
Pseudo first order	k_1 (mg/g) (min^{-1})	0.0030	0.6764
	Q_e, cal. (mg/g)	0.4669	
Pseudo-second order	k_2 (g/mg/min)	0.2380	**0.9764**
	Q_e, cal. (mg/g)	0.6477	
Elovich	α	10.5963	0.8981
	β	51.0986	

The linearized form of the Lagergren pseudo-first-order model can be presented as shown in Eq. (5) (Lagergren et al., 1898)

$$\ln(Q_e - Q_t) = lnQ_e - k_1 t \tag{5}$$

where Q_e and Q_t are equilibrium sorption capacity and amount of fluoride sorbed at time t (minutes), respectively, and k_1 is the rate constant. A plot of $\ln(Q_e - Q_t)$ against t is shown in Fig. S1 and essential kinetic parameters are given in Table 3.

A linearized form of the pseudo-second-order model is defined by Eq. (6) (Ho & McKay, 1999)

$$\frac{t}{Q_t} = \frac{1}{Q_e{}^2 k_2} + \frac{t}{Q_e} \tag{6}$$

Where and are equilibrium sorption capacity and amount of fluoride sorbed at time t (minutes) respectively, and is the rate constant. A plot of $\frac{t}{Q_t}$ against t is given in Fig. S2, and the model parameters are given in Table 3.

The non-linear form of the Elovich kinetic model is given in Eq. (7) (Roginsky & Zeldovich, 1934)

$$Q_t = \frac{1}{\beta}\ln(\alpha.\beta) + \frac{1}{\beta}\ln(t) \tag{7}$$

Where α is the initial rate at time t (minutes), and β is a parameter related to the surface coverage rate and activation energy during the chemisorption process. A plot of Q_t versus ln t is given in Fig. S3, and model parameters obtained are supplied in Table 3.

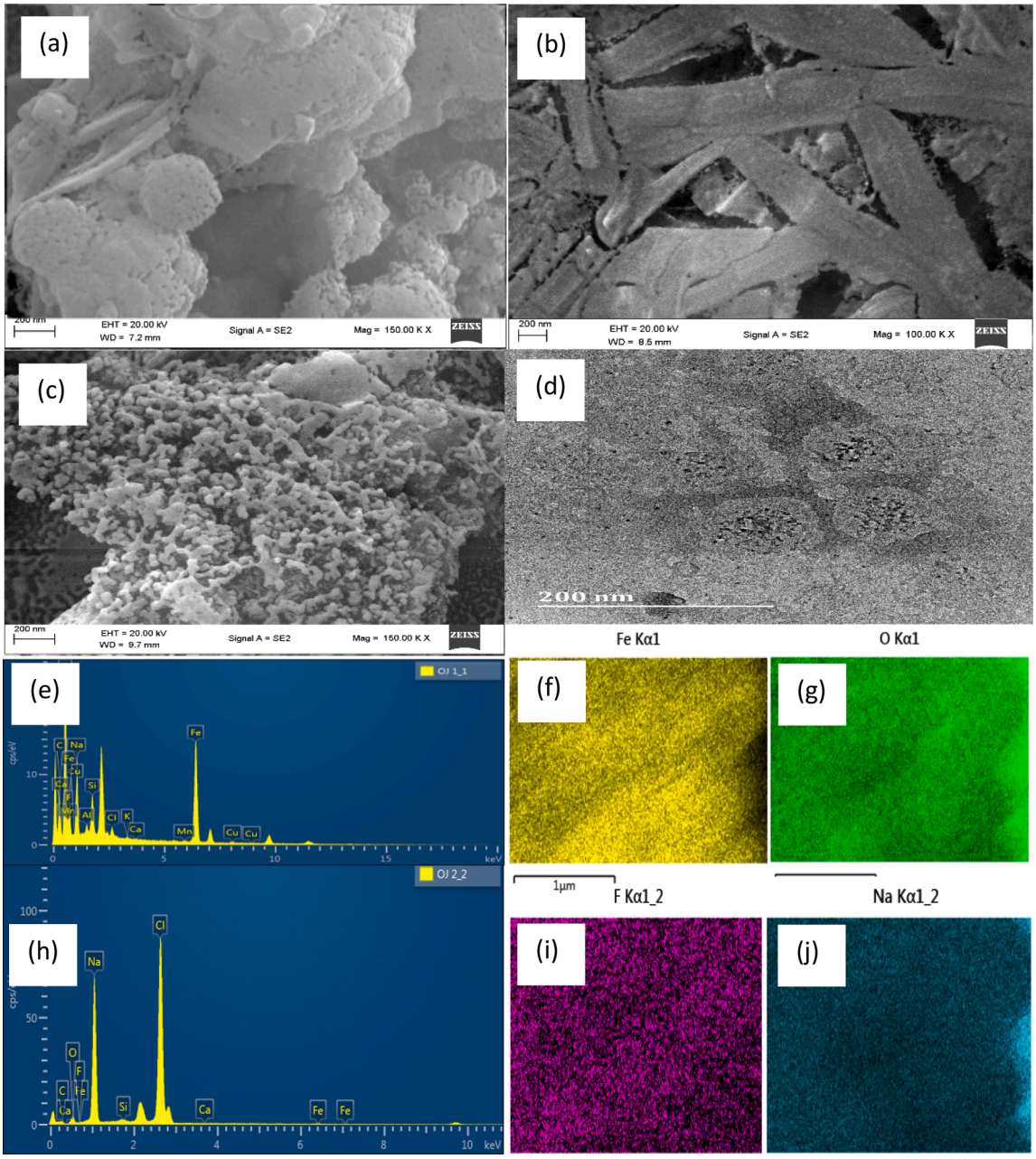

Fig 2. Microscopy images:(a) α- Fe_2O_3 composite prepared using 0 mL cassava starch, (b) α- Fe_2O_3 composite sample prepared using 10 mL cassava starch before fluoride sorption, (c) α- Fe_2O_3 composite sample prepared using 10 mL starch after fluoride sorption (d) TEM micrograph of the α- Fe_2O_3 composite sample prepared using 10 mL starch (e, h) EDX spectra and elemental mappings for the sample prepared using 10 mL of cassava starch (f, g, i, j).

The Weber-Morris intra-particle diffusion model is given in Eq. (8) (Weber & Morris, 1963)

$$Q_t = k_{id} t^{0.5} \tag{8}$$

where k_{id} is the rate constant. A plot of Q_t versus $t^{0.5}$ is given in Fig. S4, and associated model parameters are given in Table 3.

The $Q_{e,cal}$ for pseudo-second-order model is nearer to the experimental value, $Q_{e,exp}$ with an R^2 value of 0.9764. The pseudo-second-order model described fluoride sorption onto the as-synthesized α-Fe_2O_3 biocomposite. These results indicated that the sorption process is not only due to intra-particle diffusion, but other mechanisms may also be involved. Furthermore, the appearance of fluoride in the EDX spectrum after the sorption experiment signifies the sorption of fluoride onto the as-synthesized α-Fe_2O_3 biocomposite (Fig 2(h & j)).

3.5. *Model development for imitating the fluoride sorption onto α-Fe_2O_3 biocomposite*

Central composite design (CCD) was used to investigate the efficacy of fluoride sorption onto the as-synthesized α-Fe_2O_3 biocomposite. The CCD also determined the interaction between the four independent sorption process variables (initial fluoride concentration, sorbent dose, contact time, and pH) on fluoride removal efficiency. Thirty experimental runs were conducted using an experimental matrix designed using the CCD approach. In order to predict fluoride removal efficiency for varying process variable ranges, a multivariable data-driven model is explicated using analysis of variance (ANOVA) in Design-Expert Software was used. From the batch sorption experimental data obtained in this study, it was found that the variations in the fluoride sorption process can be best explained using a quadratic model shown in Eq. (9).

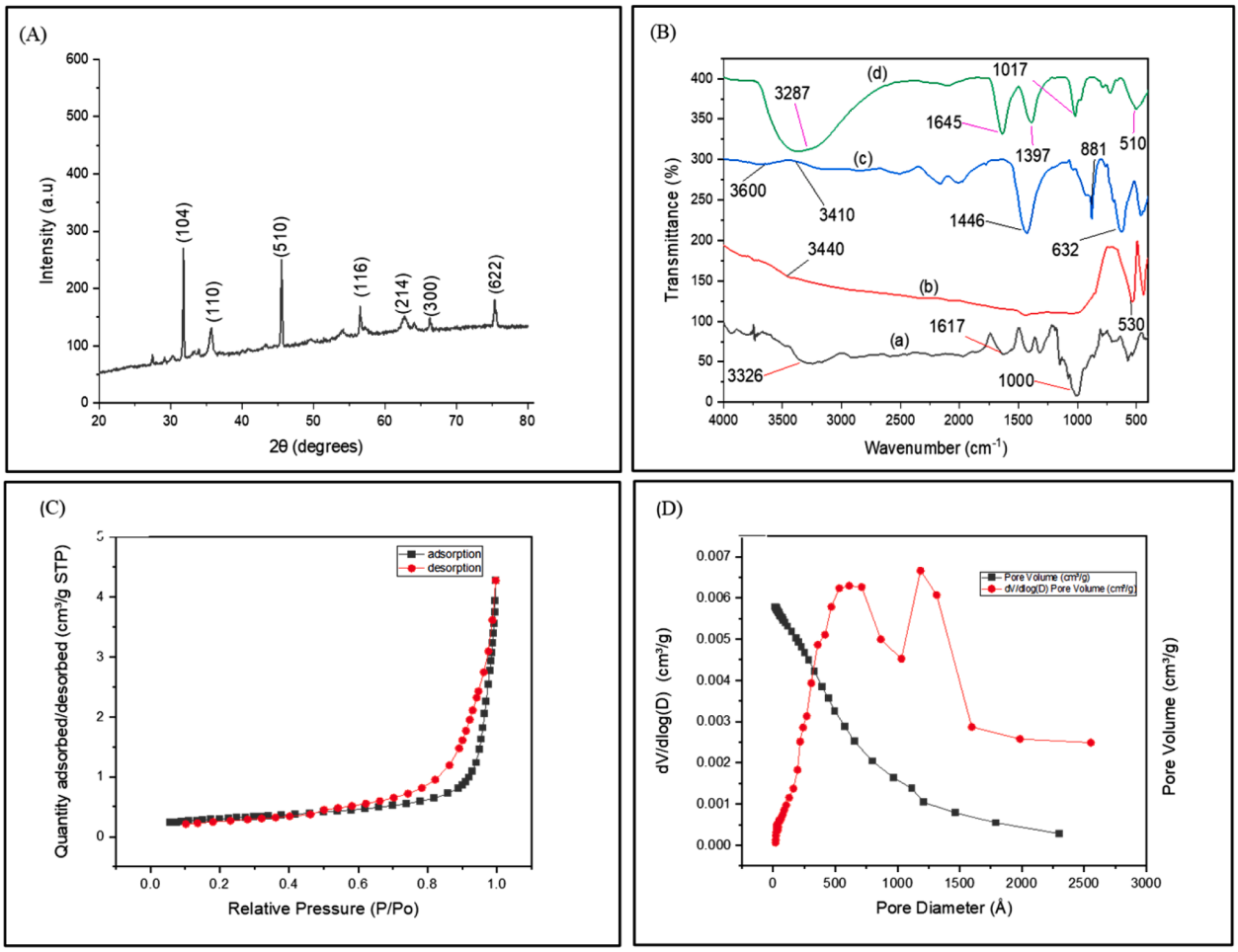

Fig 3. (A) XRD spectra of α-Fe_2O_3 biocomposite (B) FTIR spectra of (a) pristine cassava starch (CS) (b) α-Fe_2O_3-prepared using 0 CS (c) α-Fe_2O_3 biocomposite (d) α-Fe_2O_3 composite-F (C) BET plot of nitrogen adsorption-desorption for α-Fe_2O_3 biocomposite (D) pore size distribution of α-Fe_2O_3 biocomposite obtained by BJH method.

$$\text{Fluoride removal}(\%) = +5.64573 - -0.532879A + 0.742298B + 10.22384C + 12.34630D + 6.324 \times 10^{-3}D^2 - 3.131 \times 10^{-3}B^2 - -1.00093C^2 \quad (9)$$

Where the model terms are A= initial fluoride concentration (mg/L), B = contact time (minutes), C = pH, and D = sorbent dose (g/L).

The relative significance of the independent sorption process variables in model Eq. (9) was checked using p-values, F-values, R^2, lack of fit test, and good precision test.

The model F-value of 30.50 (Table 4) shows that the model is significant. Additionally, the low p-value (<0.0001) (Table 3) suggests that the model terms are similarly significant. In this study, A, B, C, D, A^2, B^2, and C^2 were significant model terms. Based on the p-values ($p < 0.05$), all four independent sorption process variables investigated in the study significantly impacted the process. Similarly, the slight difference (<0.2) between the predicted R^2 ($R^2 = 0.6747$) value and the adjusted R^2 ($R^2 = 0.8768$) value indicates that there is a good agreement between them, and the model terms are significant.

The statistical significance of the quadratic model was evaluated through an ANOVA approach, and the model was used to predict the removal of fluoride for the same sets of experimental conditions. A comparison of the response surface method (RSM) quadratic model predictions against actual experimental data is given in Fig. 5.

It can be noted that there is a strong correlation between predicted fluoride removal and actual fluoride removal, indicating that the quadratic model developed is successful in bridging the correlation between the process variables to fluoride removal efficiency using the as-synthesized α-Fe_2O_3 biocomposite.

3.6. *Effect of process parameters and their interactions on fluoride ion removal efficiency*

It is worth noting that all four independent process variables (initial fluoride concentration, contact time, pH, and sorbent dose) were recognized to influence the sorption process's efficiency (Table 4). Fig. S6 shows the effects of each parameter (A–D) on the efficiency of fluoride removal when operated singly.

It can be observed that the optimum values of the parameters are initial fluoride concentration (A = 55 mg/L), contact time (B = 95 min), pH (C = 7.5) and sorbent dosage (D = 0.55 g). The perturbation effect of each process parameter on the fluoride removal efficiency is shown in Fig.S7 (a). Notably, contact time and initial fluoride concentration

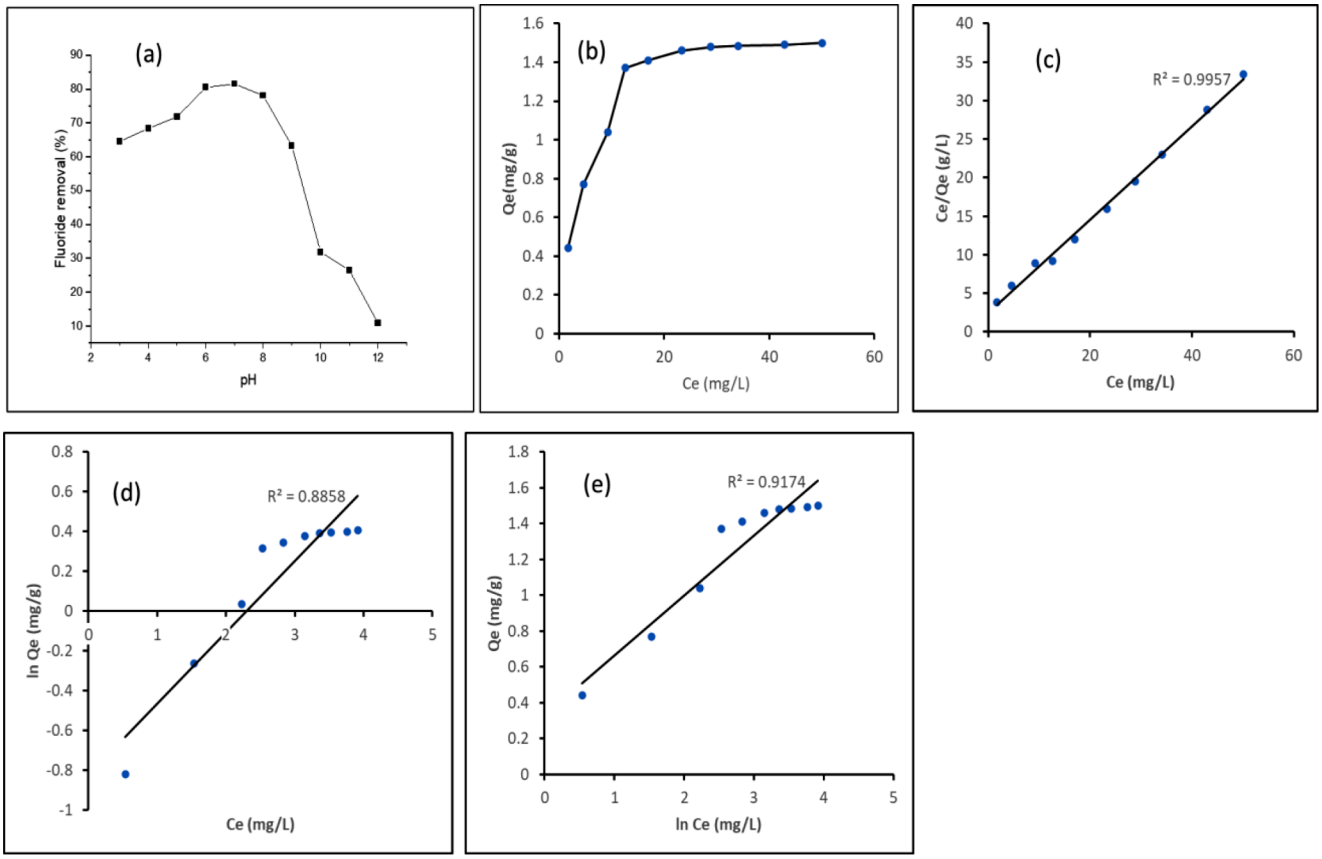

Fig. 4. Sorption equilibrium study of fluoride onto α-Fe_2O_3 biocomposite: (a) effect of pH on fluoride removal (b) variation of sorption with respect to change of the initial concentration of fluoride (c) Langmuir isotherm (d) Freundlich isotherm (e) Temkin isotherm.

Table 4
Analysis of variance (ANOVA) of quadratic model for fluoride sorption in CCD.

Source	Sum of squares	DF	Mean square	F-value	p-value	
Model	6228.41	7	889.77	30.50	< 0.0001	significant
A-Initial F^-conc.	321.86	1	321.86	11.03	0.0031	
B-Contact time	941.13	1	941.13	32.26	< 0.0001	
C-pH	2787.92	1	2787.92	95.56	< 0.0001	
D-Sorbent dose	185.20	1	185.20	6.35	0.0195	
A^2	286.99	1	286.99	9.84	0.0048	
B^2	895.72	1	895.72	30.70	< 0.0001	
C^2	718.95	1	718.95	24.64	< 0.0001	
Residual	641.85	22	29.17			
Lack of Fit	641.85	17	37.76			
Pure Error	0.0000	5	0.0000			
Cor Total	6870.26	29				

strongly influenced fluoride removal efficiency. Initial fluoride concentration below 55 mg/L resulted in low fluoride removal efficiency, while higher amounts above 55 mg/L improved fluoride removal efficiency. This increase is due to frequent interactions between the abundant fluoride ions and the as-synthesized α-Fe_2O_3 biocomposite (Raghav & Kumar, 2019). Increasing contact time(t) from 10 – 95 min improved fluoride removal efficiency. However, a further increase in contact time beyond 95 min did not improve fluoride removal due to the complete saturation of active sites on the sorbents with fluoride ions. High residence time allows for equilibration of fluoride solution with the sorbent surface and subsequent diffusion of fluoride ions into the active sites on it. Sorbent dose and pH had opposite effects, with high sorbent dose and low pH improving fluoride removal efficiency (Fig. S7(a)). These profiles, therefore, infer that each process variable has a different influence on fluoride removal efficiency when operated alone, but they exhibit interaction effects when exposed to other variables. The intrinsic characteristics of fluoride sorption onto the as-synthesized α-Fe2O3 composite in the presence of different process variables were further deciphered using the contour plots in Fig. 6 (a)-(c) and cube plots in Fig. 6 (d). The contour plots were generated by keeping two parameters constant; simultaneously, the other two were varied in their corresponding experimental runs, while cube plots considered three parameters at their center points of the design space.

To exemplify this intrinsic characteristic, when pH and sorbent dose were kept constant at 7.5 and 0.55 g, respectively, the interaction of initial fluoride concentration and contact time is shown in Fig. 6. As a result, high fluoride removal efficiency (65.12 %) was accomplished at a lower initial fluoride concentration of 32.5 mg/L and a contact time of 137.5 min (Fig. 6 (a).

Similarly, a higher fluoride percentage removal efficiency of 77.19 %

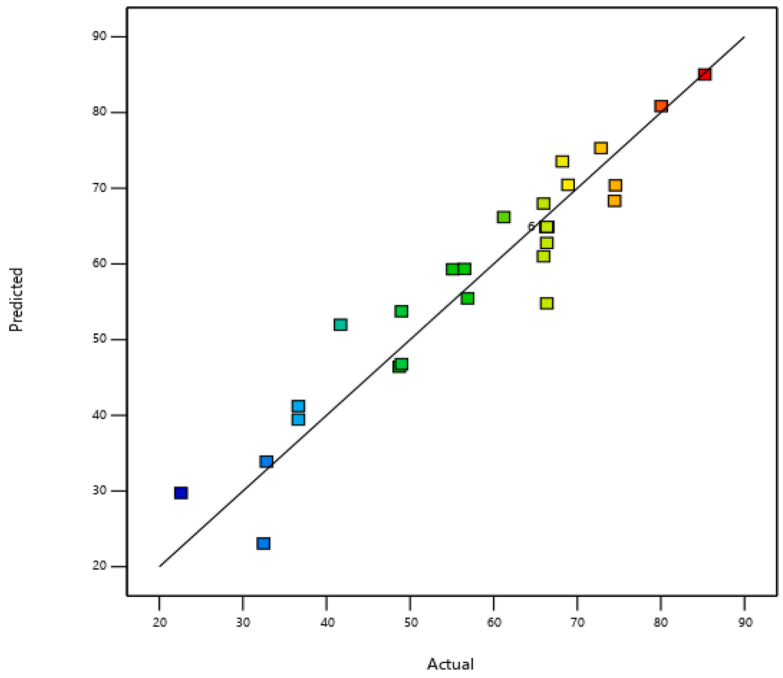

Fig. 5. Model derived and experimental graph for sorption of fluoride on as-synthesized α-Fe_2O_3 biocomposite.

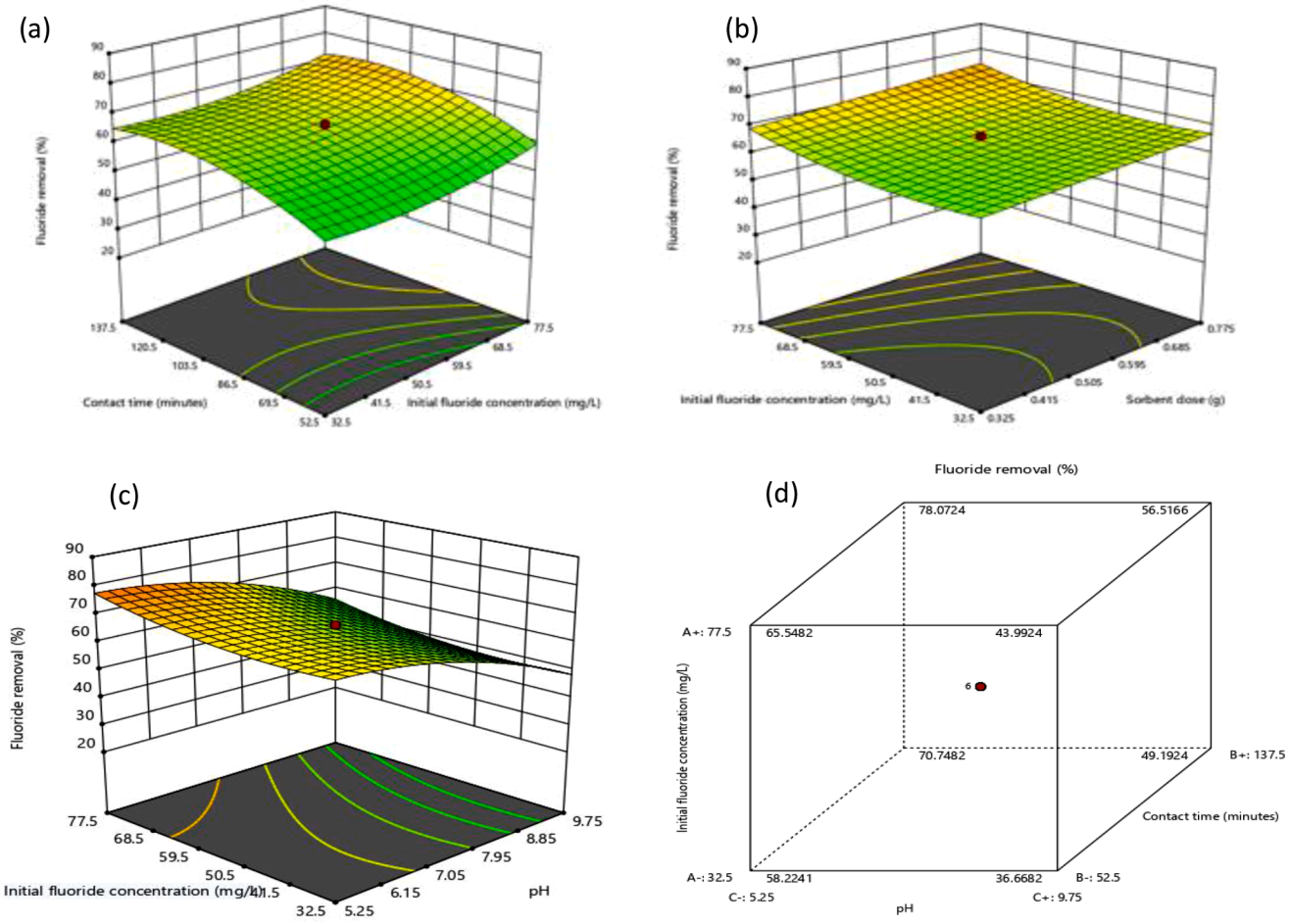

Fig. 6. . Interaction plots / 3D surface plots depicting variation in fluoride removal efficiency with: (a) initial fluoride concentration and contact time (b) initial fluoride concentration and sorbent dose (c) initial fluoride concentration and pH and (d) cube plot showing variation of fluoride removal with initial fluoride concentration - contact time - pH.

Table 5
Model validation at optimized conditions.

Sample run	Optimum parameters						
	Initial fluoride concentration (mg/L)	pH	Sorbent dose: (g)	Contact time (minutes)	Experimental fluoride removal (%)	Predicted fluoride removal (%)	STDEV
1	55.00	7.50	0.55	95.00	67.02	67.04	0.014
2	55.05	7.60	0.55	94.90	67.25	67.31	0.042
3	55.10	7.51	0.55	94.60	66.98	66.98	0.000

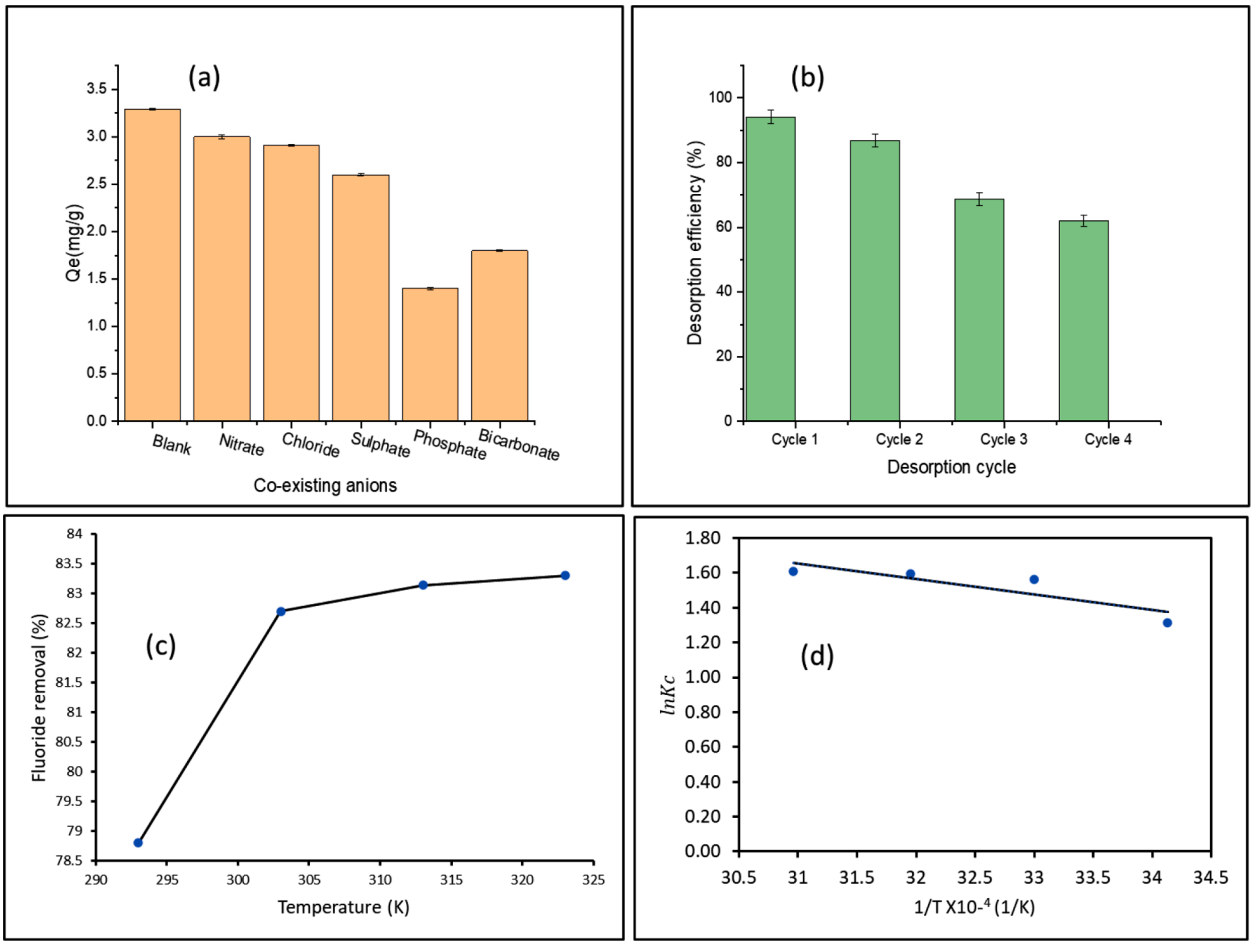

Fig. 7. (a) Effect of co-existing anions on fluoride removal using α-Fe_2O_3 biocomposite (b) Fluoride desorption efficiency from α-Fe_2O_3 biocomposite (c) Influence of temperature on fluoride removal (d)The Van't Hoff plot for the sorption of fluoride onto as-synthesized α-Fe_2O_3 biocomposite.

is attained at a lower pH value of 5.25 and a higher initial fluoride concentration of 77.50 mg/L (Fig. 6 (c)). Fluoride removal increases as a result of protonation of the sorbent surface at low pH for electrostatic attraction of fluoride ions. Fig. 6(b) displays an interaction plot of sorbent dose and initial fluoride concentration. It can be appreciated that a high percentage of fluoride removal of 69.02 % can be accomplished at a lower sorbent dose (0.325 g) and higher initial fluoride concentration of 77.50 mg/L. Three-factor interactions are presented in Fig. 6(d) and Fig S7(d).

The fluoride removal efficiency of 66.36 % can be achieved by using a lower sorbent dose of 0.55 g, initial fluoride concentration of 55 mg/L, and contact time of 95 min. However, increasing the magnitude of the parameters above these values can improve percentage fluoride removal efficiency up to 75.14 %, provided pH remains constant at 7.5.

Similar trends are shown in Fig. S 7 (d), where fluoride removal efficiency of 78.07 % can be achieved by keeping sorbent dose at 0.55 g and increasing initial fluoride concentration from 32.5 to 77.5 mg/L, contact time from 52.5 to 137.5 min, and pH from 5.25 to 7.5.

However, an increase in pH beyond 8 can lead to decreased percentage of fluoride removal even if other factors are increased due to the electrostatic repulsion between fluoride ions and hydroxide ions introduced at high pH. Finally, Fig. S7 displays a similar trend of increasing fluoride removal efficiency with an increase in process variables in the pH range 5.25 - 8, as observed in the interaction plot of initial fluoride concentration-contact time-pH.

3.7. Process optimization and model validation

The optimal values of the process variables for maximum fluoride removal of 85.26 % by the as-synthesized α-Fe_2O_3 biocomposite were an initial fluoride concentration of 55 mg/L, sorbent dose of 0.55 g, contact time of 95 min, and a pH of 7.5 (Fig.S6).

Three of the optimized conditions were selected to conduct experiments to validate the model. The experiments were repeated to verify the prediction, and the results are given in Table 5. It was observed that the experimental values of fluoride removal are in good agreement with

the model predicted values with a standard error < 0.05.

3.8. Sorption thermodynamics

Batch sorption experiments investigated the effect of temperature on fluoride removal by as-synthesized α-Fe_2O_3 biocomposite at temperatures ranging from 298 K to 323 K using an initial fluoride concentration of 10 mg/L in order to decipher information regarding the sorption process. The thermodynamic parameters obtained from the Van't Hoff plot Fig. 7(a) and thermodynamic relations (Eqs. 10 – (12) are summarized in Table 5

$$lnK_c = -\frac{\Delta H}{R}\left[\frac{1}{T}\right] + \frac{\Delta S}{R} \quad (10)$$

$$\Delta G = -RTlnK_c \quad (11)$$

$$K_c = \frac{C_{ad}}{C_e} \quad (12)$$

where K_c, ΔH (J/mol), R (8.314 J/mol K), T (K), ΔS (J/mol/K), ΔG (J/mol.K), C_e (mg/L), and C_{ad} (mg/L) are the equilibrium constant, enthalpy change, molar gas constant, absolute temperature, entropy change, Gibbs free energy change, the concentration of fluoride ions in solution at equilibrium and amount of fluoride sorbed onto as-synthesized α-Fe_2O_3 biocomposite at equilibrium, respectively.

The negative value of ΔH signified an exothermic process, and the positive value of ΔS showed that the randomness at the solid/liquid interface increased during the sorption process. Furthermore, the values obtained became more positive when the temperature was increased, indicating that the sorption of fluoride onto the as-synthesized α-Fe_2O_3 biocomposite was feasible and spontaneous (Raghav & Kumar, 2019).

Lastly, it is a valuable source of information regarding the description of the sorption process. Generally, values in the range −20 – 0 kJ/mol indicate physisorption, while those in the range −400 – −80 kJ/mol show chemisorption process (Raghav & Kumar, 2019). In the present study, values obtained fall in the range of −20 – 0 kJ/mol, confirming that the fluoride removal by the as-synthesized α-Fe_2O_3 composite involved the physisorption process.

3.9. Desorption and reusability study

The regeneration and recovery of the spent sorbent is a vital indicator to appraise the performance of the as-synthesized α-Fe_2O_3 biocomposite for sustainable remediation of fluoride-ladened water (Egor et al., 2021; Prabhu & Meenakshi, 2015; Raghav & Kumar, 2019). In this study, spent sorbent was regenerated in four cycles by desorption using a 0.1 M sodium hydroxide solution. Unfortunately, the efficiency of the desorption in each cycle decreased, as shown in Fig. 7 (b) ($p < 0.05$). Nevertheless, the composite still had 62 % effectiveness for fluoride removal in the fourth cycle. Therefore, the as-synthesized α-Fe_2O_3 biocomposite can be a reusable sorbent for the remediation of fluoride-ladened water.

3.10. Leaching tests for Fe and stability test

The amount of Fe leached into the treated water was appraised using a Perkin Elmer Optima 7300 DV Inductively Coupled Plasma- Optical Emission Spectrometer (ICP-OES). Deionized water before and after contact with the composite was acidified with 5% nitric acid prior to measurement of Fe in a precalibrated Perkin Elmer ICP-OES following the standard US EPA method 200.7. The amount of Fe leached into the water was 0.01–0.1 mg/L and 0.06–0.2 mg/L, respectively, below the WHO (2017) limits for drinking water. The leaching tests further indicate that the metal hydroxides/ oxyhydroxides were incorporated in the starch polymer cages and, so, not easily leached into the water.

3.11. Effect of co-existing anions on fluoride removal using α-Fe_2O_3 composite

The effect of co-existing anions: NO_3^-, Cl^-, SO_4^{2-}, PO_4^{3-} and HCO_3^-, which commonly occur in natural water, on fluoride removal using α-Fe_2O_3 biocomposite, was investigated in this study and were compared against a blank (fluoride solution without other salts) (Fig. 7 (a). As presented in Fig. 7 (a), the presence of the five anions negatively affected the fluoride removal capacity of the as-synthesized α-Fe_2O_3 biocomposite. The addition of NO_3^-, Cl^-, and SO_4^{2-} had a slight negative effect, while the addition of PO_4^{3-} and HCO_3^- reduced the fluoride removal potential of the composite considerably. This phenomenon is because of the anions' charge density (Z/r_a). The strength of the influence of these anions was in the order PO_4^{3-} (3/2.38) > HCO_3^- (1/1.56) > SO_4^{2-} (2/2.30) > NO_3^- (1/1.79) > Cl^- (1/1.81)(Cotton et al., 1988). Notably, PO_4^{3-} with the highest anionic charge density, had the greatest influence suggesting the sorbent's active site can preferentially take it up instead of fluoride with a lower charge density (Z/ra = 1/1.33). For HCO_3^- ion, its influence may be due to a similar charge density as F^- ions. SO_4^{2-} ion showed a slight effect, probably due to its large radius, whereas NO_3^- and Cl^- only showed a slight effect due to their inferior ability to bind with active sites on the sorbent. The result is consistent with reports from other studies that found similar interference trends by co-existing anions(Mondal & Purkait, 2019).

4. Conclusions

A facile green synthesis of α-Fe_2O_3 biocomposite as a novel sorbent for fluoride removal mediated by cassava starch obtained from cassava waste was achieved in this study. Characterization of as-synthesized composite achieved using powder XRD, SEM-EDS, TEM-EDS, and Micrometric Tristar II surface area and porosity analyzer revealed that the composite is hard and contains porous α-Fe_2O_3 particles. Furthermore, the composite is stable in water with minimal leaching of metals under the conditions of use, effectively scavenging fluoride ions at pH 6–8 with diminished efficiency in the presence of PO_4^{3-} and HCO_3^-.

Response surface methodology proved to be a suitable tool for modeling and optimizing conditions for fluoride removal using α-Fe_2O_3 biocomposite. Analysis of variance (ANOVA) provided a quadratic model with a model F-value of 30.50 and $p < 0.0001$ demonstrating the high significance of the model. In addition, the model predictions with a high regression coefficient ($R^2 = 0.9066$) further indicate good model performance. Based on the ANOVA results, optimum conditions to attain 85.26 % fluoride removal efficiency were a sorbent dose of 0.55 g, initial fluoride concentration of 55 mg/L, pH value of 7.5 and contact time of 95 min. The contour plot revealed that the most substantial interaction occurred between initial fluoride concentration and contact time.

The sorption equilibrium isotherm was multilayered on a heterogeneous surface of the sorbent with a varied affinity for fluoride. At the same time, its kinetics was better modeled by pseudo-second-order kinetics ($R^2 = 0.9764$), showing that the sorption process is rate-limiting. From the thermodynamic parameters obtained, fluoride sorption toward as-synthesized α-Fe_2O_3 biocomposite was a spontaneous, exothermic, entropy-driven process. From the sorption study, the as-synthesized α-Fe_2O_3 composite mediated by cassava starch can be a potential sorbent for removing fluoride and other contaminants in water (Table 6).

Table 6
Sorption thermodynamic parameters for the removal of fluoride by as-synthesized α-Fe_2O_3 composite.

ΔH(J/mol)	ΔS(J/mol/K)	ΔG(kJ/mol)				
		293 K	303 K	313 K	323 K	R^2
−0.732	36.413	−8.599	−8.808	−9.014	−9.218	0.9998

Declaration of Competing Interest

The authors declare that they have no known competing financial interests or personal relationships which have or could be perceived to have influenced the work reported in this article.

Acknowledgment

The authors gratefully acknowledge the African-German Network of Excellence in Science (AGNES) and the German Academic Exchange Service (DAAD) [Grant number: 91672385] for funding the study.This work was also supported in part by the Danvera Foundation (Bolender). In addition, the authors are grateful for the instrumentation and technical support from the School of Chemistry and Physics, University of KwaZulu-Natal, Westville Campus, Durban in South Africa, and the Department of Chemistry, Mbarara University of Science and Technology, Mbarara in Uganda.

Supplementary materials

Supplementary material associated with this article can be found, in the online version, at doi:10.1016/j.carpta.2022.100241.

References

Abbo, H. S., Gupta, K. C., Khaligh, N. G., & Titinchi, S. J. J. (2021). Carbon nanomaterials for wastewater treatment. *ChemBioEng Reviews, 8*(5), 463–489.

Alhassan, S. I., Huang, L., He, Y., Yan, L., Wu, B., & Wang, H. (2020). Fluoride removal from water using alumina and aluminum-based composites: A comprehensive review of progress. *Critical Reviews in Environmental Science and Technology*, 1–35.

Biswas, K., Gupta, K., & Ghosh, U. C. (2009). Adsorption of fluoride by hydrous iron (III)–tin (IV) bimetal mixed oxide from the aqueous solutions. *Chemical Engineering Journal, 149*(1–3), 196–206.

Cotton, F. A., Wilkinson, G., Murillo, C. A., Bochmann, M., & Grimes, R. (1988). *Advanced inorganic chemistry, 5*. Wiley New York.

Dehghani, M. H., Gholami, S., Karri, R. R., Lima, E. C., Mahvi, A. H., Nazmara, S., & Fazlzadeh, M. (2021). Process modeling, characterization, optimization, and mechanisms of fluoride adsorption using magnetic agro-based adsorbent. *Journal of Environmental Management, 286*, Article 112173.

Egor, M., Kumar, A. A., Ahuja, T., Mukherjee, S., Chakraborty, A., Sudhakar, C., Srikrishnarka, P., Bose, S., Ravindran, S. J., & Pradeep, T. (2021). Cellulosic ternary nanocomposite for affordable and sustainable fluoride removal. *ACS Sustainable Chemistry & Engineering, 9*(38), 12788–12799.

Erdal, S., & Buchanan, S. N. (2005). A quantitative look at fluorosis, fluoride exposure, and intake in children using a health risk assessment approach. *Environmental Health Perspectives, 113*(1), 111–117.

Fardood, S.T., Ramazani, A., Golfar, Z., & Joo, S.W. (2017). Green synthesis of α-Fe 2 O 3 (hematite) nanoparticles using tragacanth gel.

Everett, D. H., Parfitt, G. D., Sing, K. S., & Wilson, R. (1974). The SCI/IUPAC/NPL project on surface area standards. *Journal of Applied Chemistry and Biotechnology, 24*(4–5), Article 199-219-24.

Freundlich, H. M. F. (1906). Over the adsorption in solution. *J. Phys. chem, 57*(385471), 1100–1107.

Gasparotto, J. M., Roth, D., Perilli, A. L., de, O., Franco, D. S. P., Carissimi, E., Foletto, E. L., Jahn, S. L., & Dotto, G. L. (2021). A novel Fe-Al-La trioxide composite: Synthesis, characterization, and application for fluoride ions removal from the water supply. *Journal of Environmental Chemical Engineering*, (6), 9. https://doi.org/10.1016/j.jece.2021.106350

Gautam, P.K., Pingali, S., & Sahoo, A.K. (2019). Biogenic fabrication of iron nanoadsorbents from mixed waste biomass for aqueous phase removal of alizarin red S and tartrazine : Kinetics, isotherm, and thermodynamic investigation. January 2020. https://doi.org/10.1002/ep.13326.

Gogoi, C., Saikia, J., Sarmah, S., Sinha, D., & Goswamee, R. L. (2018). Removal of fluoride from water by locally available sand modified with a coating of iron oxides. *Water, Air, & Soil Pollution, 229*(4), 1–16.

Gupta, A. D., Rawat, K. P., Bhadauria, V., & Singh, H. (2021). Recent trends in the application of modified starch in the adsorption of heavy metals from water: A review. *Carbohydrate Polymers, 269*, Article 117763.

He, J., Yang, Y., Wu, Z., Xie, C., Zhang, K., Kong, L., & Liu, J. (2020). Review of fluoride removal from water environment by adsorption. *Journal of Environmental Chemical Engineering, 8*(6), Article 104516.

Hegde, R. M., Rego, R. M., Potla, K. M., Kurkuri, M. D., & Kigga, M. (2020). Bio-inspired materials for defluoridation of water: A review. *Chemosphere*, Article 126657.

Ho, Y.-S., & McKay, G. (1999). Pseudo-second order model for sorption processes. *Process Biochemistry, 34*(5), 451–465.

Hoque, M. I. U., Yamauchi, Y., Naidu, R., Holze, R., Saidur, R., Qu, Q., Rahman, M. M., Torad, N. L., Hossain, M. S. A., Kim, M., Kim, J., Ahmad, S. H. A., Rehman, A. U., Firoz, M. S. H., Luba, U., Chowdhury, S., & Chowdhury, A. N. (2019). A facile synthesis of hematite nanorods from rice starch and their application to Pb(II) ions removal. *Chemistry Select, 4*(13), 3730–3736. https://doi.org/10.1002/slct.201802462

Kumar, E., Bhatnagar, A., Ji, M., Jung, W., Lee, S.-H., Kim, S.-J., Lee, G., Song, H., Choi, J.-Y., & Yang, J.-S. (2009). Defluoridation from aqueous solutions by granular ferric hydroxide (GFH). *Water Research, 43*(2), 490–498.

Lagergren, S., Lagergren, S., Lagergren, S.Y., & Sven, K. (1898). Zurtheorie der sogenannten adsorption gelösterstoffe.

Langmuir, I. (1918). The adsorption of gases on plane surfaces of glass, mica and platinum. *Journal of the American Chemical society, 40*(9), 1361–1403.

Lingamdinne, L. P., Vemula, K. R., Chang, Y.-Y., Yang, J.-K., Karri, R. R., & Koduru, J. R. (2020). Process optimization and modeling of lead removal using iron oxide nanocomposites generated from bio-waste mass. *Chemosphere, 243*, Article 125257.

Mahfoudhi, N., & Boufi, S. (2020). Porous material from cellulose nanofibrils coated with aluminum hydroxyde as an effective adsorbent for fluoride. *Journal of Environmental Chemical Engineering, 8*(3), Article 103779. https://doi.org/10.1016/j.jece.2020.103779

Mondal, P., & Purkait, M. K. (2019). Preparation and characterization of novel green synthesized iron–Aluminum nanocomposite and studying its efficiency in fluoride removal. *Chemosphere, 235*, 391–402.

Mumtaz, N., Pandey, G., & Labhasetwar, P. K. (2015). Global fluoride occurrence, available technologies for fluoride removal, and electrolytic defluoridation: a review. *Critical Reviews in Environmental Science and Technology, 45*(21), 2357–2389.

Murambasvina, G., & Mahamadi, C. (2020). Effective fluoride adsorption using water hyacinth beads doped with hydrous oxides of aluminium and iron. *Groundwater for Sustainable Development, 10*, Article 100302.

Ojok, W., Wanasolo, W., Wasswa, J., Bolender, J., & Ntambi, E. (2021). Hydrochemistry and fluoride contamination in Ndali-Kasenda crater lakes, Albertine Graben: Assessment based on multivariate statistical approach and human health risk. *Groundwater for Sustainable Development*, Article 100650.

Pandi, K., Periyasamy, S., & Viswanathan, N. (2017). Remediation of fluoride from drinking water using magnetic iron oxide coated hydrotalcite/chitosan composite. *International Journal of Biological Macromolecules, 104*, 1569–1577. https://doi.org/10.1016/j.ijbiomac.2017.02.037

Pillai, P., Dharaskar, S., Sinha, M. K., Sillanpää, M., & Khalid, M. (2020). Iron oxide nanoparticles modified with ionic liquid as an efficient adsorbent for fluoride removal from groundwater. *Environmental Technology & Innovation*, Article 100842.

Prabhu, S. M., & Meenakshi, S. (2015). Novel one-pot synthesis of dicarboxylic acids mediated alginate–Zirconium biopolymeric complex for defluoridation of water. *Carbohydrate Polymers, 120*, 60–68.

Raghav, S., & Kumar, D. (2019). Comparative kinetics and thermodynamic studies of fluoride adsorption by two novel synthesized biopolymer composites. *Carbohydrate Polymers, 203*, 430–440.

Roginsky, S., & Zeldovich, Y. B. (1934). The catalytic oxidation of carbon monoxide on manganese dioxide. *Acta Physicochimica Chem USSR, 1*(554), 2019.

Sarkar, S., Guibal, E., Quignard, F., & SenGupta, A. K. (2012). Polymer-supported metals and metal oxide nanoparticles: synthesis, characterization, and applications. *Journal of Nanoparticle Research, 14*(2), 1–24.

Sasireka, K. S., & Lalitha, P. (2021). Biogenic synthesis of bimetallic nanoparticles and their applications. *Reviews in Inorganic Chemistry*.

Shah, N., Khan, W. A., Rehan, T., Lin, D., Tetik, H., & Haider, S (2022). 12 - Polysaccharides-metal oxide composite: A green functional material. S. Haider & A. B. T.-R. P. and P.-M. O. C. Haider (Eds.). *Metal oxides* (pp. 371–394). Elsevier. https://doi.org/10.1016/B978-0-323-85155-8.00013-3.

Singh, J., Dutta, T., Kim, K.-H., Rawat, M., Samddar, P., & Kumar, P. (2018). 'Green'synthesis of metals and their oxide nanoparticles: Applications for environmental remediation. *Journal of Nanobiotechnology, 16*(1), 1–24.

Tang, Q., Duan, T., Li, P., Zhang, P., & Wu, D. (2018). Enhanced defluoridation capacity from aqueous media via hydroxyapatite decorated with carbon nanotube. *Frontiers in Chemistry, 6*, 104.

Tefera, N., Mulualem, Y., & Fito, J. (2020). Adsorption of fluoride from aqueous solution and groundwater onto activated carbon of avocado seeds. *Water Conservation Science and Engineering, 5*(3), 187–197. https://doi.org/10.1007/s41101-020-00093-7

Temkin, M.J., & Pyzhev, V. (1940). Recent modifications to Langmuir isotherms.

Visinescu, D., Tirsoaga, A., Patrinoiu, G., Tudose, M., Paraschiv, C., Ianculescu, A., & Carp, O. (2010). Green synthetic strategies of oxide materials: Polysaccharides-assisted synthesis. *Revue Roumaine de Chimie, 55*(11–12), 1017–1026.

Wang, H. (2020). Fluoride removal from water using alumina and aluminum-based composites : A comprehensive review of progress. *Critical Reviews in Environmental Science and Technology*, 1–35. https://doi.org/10.1080/10643389.2020.1769441. *0* (0).

Weber, W. J., & Morris, J. C. (1963). Kinetics of adsorption on carbon from solution. *Journal of the Sanitary Engineering Division, 89*(2), 31–60.

Xu, L., Chen, G., Peng, C., Qiao, H., Ke, F., & Hou, R. (2017). Adsorptive removal of fluoride from drinking water using porous starch loaded with common metal ions Adsorptive removal of fluoride from drinking water using porous starch loaded with common metal ions. *Carbohydrate Polymers, 160*(March), 82–89. https://doi.org/10.1016/j.carbpol.2016.12.052

Xu, L., Chen, G., Peng, C., Qiao, H., Ke, F., Hou, R., Li, D., Cai, H., & Wan, X. (2017). Adsorptive removal of fluoride from drinking water using porous starch loaded with common metal ions. *Carbohydrate Polymers, 160*, 82–89.

Zhang, C., Li, Y., Wang, T.-J., Jiang, Y., & Wang, H. (2016). Adsorption of drinking water fluoride on a micron-sized magnetic Fe3O4@ Fe-Ti composite adsorbent. *Applied Surface Science, 363*, 507–515.